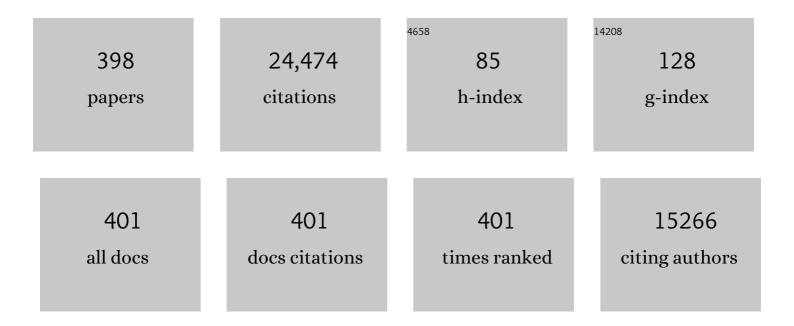
List of Publications by Year in descending order

Source: https://exaly.com/author-pdf/1572843/publications.pdf Version: 2024-02-01



#	Article	IF	CITATIONS
1	Removal of basic dye Auramine-O by ZnS:Cu nanoparticles loaded on activated carbon: optimization of parameters using response surface methodology with central composite design. RSC Advances, 2015, 5, 18438-18450.	3.6	650
2	Modeling of competitive ultrasonic assisted removal of the dyes – Methylene blue and Safranin-O using Fe3O4 nanoparticles. Chemical Engineering Journal, 2015, 268, 28-37.	12.7	570
3	Simultaneous preconcentration and determination of copper, nickel, cobalt and lead ions content by flame atomic absorption spectrometry. Journal of Hazardous Materials, 2007, 142, 272-278.	12.4	429
4	Hydrophilic Multitemplate Molecularly Imprinted Biopolymers Based on a Green Synthesis Strategy for Determination of B-Family Vitamins. ACS Applied Materials & Interfaces, 2018, 10, 4140-4150.	8.0	310
5	Dummy molecularly imprinted polymers based on a green synthesis strategy for magnetic solid-phase extraction of acrylamide in food samples. Talanta, 2019, 195, 390-400.	5.5	302
6	Optimization of the ultrasonic assisted removal of methylene blue by gold nanoparticles loaded on activated carbon using experimental design methodology. Ultrasonics Sonochemistry, 2014, 21, 242-252.	8.2	270
7	Cloud point extraction and flame atomic absorption spectrometric determination of cadmium(II), lead(II), palladium(II) and silver(I) in environmental samples. Journal of Hazardous Materials, 2009, 168, 1022-1027.	12.4	267
8	Ultrasonically assisted hydrothermal synthesis of activated carbon–HKUST-1-MOF hybrid for efficient simultaneous ultrasound-assisted removal of ternary organic dyes and antibacterial investigation: Taguchi optimization. Ultrasonics Sonochemistry, 2016, 31, 383-393.	8.2	267
9	Multiwalled Carbon Nanotubes as Adsorbents for the Kinetic and Equilibrium Study of the Removal of Alizarin Red S and Morin. Journal of Chemical & Engineering Data, 2011, 56, 2511-2520.	1.9	245
10	Modeling of quaternary dyes adsorption onto ZnO–NR–AC artificial neural network: Analysis by derivative spectrophotometry. Journal of Industrial and Engineering Chemistry, 2016, 34, 186-197.	5.8	240
11	Carbon based materials: a review of adsorbents for inorganic and organic compounds. Materials Advances, 2021, 2, 598-627.	5.4	232
12	Response surface methodology approach for optimization of simultaneous dye and metal ion ultrasound-assisted adsorption onto Mn doped Fe ₃ O ₄ -NPs loaded on AC: kinetic and isothermal studies. Dalton Transactions, 2015, 44, 14707-14723.	3.3	230
13	Development of a Lower Toxic Approach Based on Green Synthesis of Water-Compatible Molecularly Imprinted Nanoparticles for the Extraction of Hydrochlorothiazide from Human Urine. ACS Sustainable Chemistry and Engineering, 2017, 5, 3775-3785.	6.7	219
14	Comparison of silver and palladium nanoparticles loaded on activated carbon for efficient removal of Methylene blue: Kinetic and isotherm study of removal process. Powder Technology, 2012, 228, 18-25.	4.2	206
15	Sonochemical-assisted synthesis of CuO/Cu2O/Cu nanoparticles as efficient photocatalyst for simultaneous degradation of pollutant dyes in rotating packed bed reactor: LED illumination and central composite design optimization. Ultrasonics Sonochemistry, 2018, 40, 601-610.	8.2	202
16	Highly Selective and Sensitive Preconcentration of Mercury Ion and Determination by Cold Vapor Atomic Absorption Spectroscopy. Analytical Letters, 2006, 39, 1171-1185.	1.8	200
17	Optimization of the combined ultrasonic assisted/adsorption method for the removal of malachite green by gold nanoparticles loaded on activated carbon: Experimental design. Spectrochimica Acta - Part A: Molecular and Biomolecular Spectroscopy, 2014, 118, 55-65.	3.9	191
18	Novel strategy for synthesis of magnetic dummy molecularly imprinted nanoparticles based on functionalized silica as an efficient sorbent for the determination of acrylamide in potato chips: Optimization by experimental design methodology. Talanta, 2016, 154, 526-532.	5.5	186

#	Article	IF	CITATIONS
19	The determination of some heavy metals in food samples by flame atomic absorption spectrometry after their separation-preconcentration on bis salicyl aldehyde, 1,3 propan diimine (BSPDI) loaded on activated carbon. Journal of Hazardous Materials, 2008, 154, 128-134.	12.4	183
20	Simultaneous ultrasound-assisted ternary adsorption of dyes onto copper-doped zinc sulfide nanoparticles loaded on activated carbon: Optimization by response surface methodology. Spectrochimica Acta - Part A: Molecular and Biomolecular Spectroscopy, 2015, 145, 203-212.	3.9	182
21	Synthesis of magnetic γ-Fe2O3-based nanomaterial for ultrasonic assisted dyes adsorption: Modeling and optimization. Ultrasonics Sonochemistry, 2016, 32, 418-431.	8.2	174
22	Statistical experimental design, least squares-support vector machine (LS-SVM) and artificial neural network (ANN) methods for modeling the facilitated adsorption of methylene blue dye. RSC Advances, 2016, 6, 40502-40516.	3.6	168
23	Screening and optimization of highly effective ultrasound-assisted simultaneous adsorption of cationic dyes onto Mn-doped Fe3O4-nanoparticle-loaded activated carbon. Ultrasonics Sonochemistry, 2017, 34, 1-12.	8.2	165
24	Comparative study on ultrasonic assisted adsorption of dyes from single system onto Fe3O4 magnetite nanoparticles loaded on activated carbon: Experimental design methodology. Ultrasonics Sonochemistry, 2017, 34, 294-304.	8.2	164
25	Highly efficient simultaneous ultrasonic assisted adsorption of brilliant green and eosin B onto ZnS nanoparticles loaded activated carbon: Artificial neural network modeling and central composite design optimization. Spectrochimica Acta - Part A: Molecular and Biomolecular Spectroscopy, 2016, 153, 257-267.	3.9	160
26	Development of dummy molecularly imprinted based on functionalized silica nanoparticles for determination of acrylamide in processed food by matrix solid phase dispersion. Food Chemistry, 2016, 210, 78-84.	8.2	156
27	The performance of nanorods material as adsorbent for removal of azo dyes and heavy metal ions: Application of ultrasound wave, optimization and modeling. Ultrasonics Sonochemistry, 2017, 34, 792-802.	8.2	153
28	Application of central composite design for simultaneous removal of methylene blue and Pb2+ ions by walnut wood activated carbon. Spectrochimica Acta - Part A: Molecular and Biomolecular Spectroscopy, 2015, 135, 479-490.	3.9	149
29	Ultrasonic enhancement of the simultaneous removal of quaternary toxic organic dyes by CuO nanoparticles loaded on activated carbon: Central composite design, kinetic and isotherm study. Ultrasonics Sonochemistry, 2016, 31, 546-557.	8.2	149
30	Magnetic nanoparticle based dispersive micro-solid-phase extraction for the determination of malachite green in water samples: optimized experimental design. New Journal of Chemistry, 2015, 39, 9813-9823.	2.8	146
31	Experimental design based response surface methodology optimization of ultrasonic assisted adsorption of safaranin O by tin sulfide nanoparticle loaded on activated carbon. Spectrochimica Acta - Part A: Molecular and Biomolecular Spectroscopy, 2014, 122, 223-231.	3.9	145
32	Preparation and Characterization of Mn _{0.4} Zn _{0.6} Fe ₂ O ₄ Nanoparticles Supported on Dead Cells of <i>Yarrowia lipolytica</i> as a Novel and Efficient Adsorbent/Biosorbent Composite for the Removal of Azo Food Dyes: Central Composite Design Optimization Study. ACS Sustainable Chemistry	6.7	142
33	and Engineering, 2018, 6, 4549-4563. Application of machine/statistical learning, artificial intelligence and statistical experimental design for the modeling and optimization of methylene blue and Cd(<scp>ii</scp>) removal from a binary aqueous solution by natural walnut carbon. Physical Chemistry Chemical Physics, 2017, 19, 11299-11317.	2.8	141
34	Photocatalytic degradation of binary mixture of toxic dyes by HKUST-1 MOF and HKUST-1-SBA-15 in a rotating packed bed reactor under blue LED illumination: central composite design optimization. RSC Advances, 2016, 6, 17204-17214.	3.6	140
35	Ultrasound-assisted binary adsorption of dyes onto Mn@ CuS/ZnS-NC-AC as a novel adsorbent: Application of chemometrics for optimization and modeling. Journal of Industrial and Engineering Chemistry, 2017, 54, 377-388.	5.8	137
36	Preparation of low cost activated carbon from Myrtus communis and pomegranate and their efficient application for removal of Congo red from aqueous solution. Spectrochimica Acta - Part A: Molecular and Biomolecular Spectroscopy, 2012, 86, 107-114.	3.9	136

#	Article	IF	CITATIONS
37	Rapid removal of Auramine-O and Methylene blue by ZnS:Cu nanoparticles loaded on activated carbon: A response surface methodology approach. Journal of the Taiwan Institute of Chemical Engineers, 2015, 53, 80-91.	5.3	136
38	Sonophotocatalytic degradation of trypan blue and vesuvine dyes in the presence of blue light active photocatalyst of Ag3PO4/Bi2S3-HKUST-1-MOF: Central composite optimization and synergistic effect study. Ultrasonics Sonochemistry, 2016, 32, 387-397.	8.2	136
39	Rapid ultrasound-assisted magnetic microextraction of gallic acid from urine, plasma and water samples by HKUST-1-MOF-Fe3O4-GA-MIP-NPs: UV–vis detection and optimization study. Ultrasonics Sonochemistry, 2017, 34, 561-570.	8.2	132
40	Enhanced simultaneous removal of malachite green and safranin O by ZnO nanorod-loaded activated carbon: modeling, optimization and adsorption isotherms. New Journal of Chemistry, 2015, 39, 7998-8005.	2.8	130
41	Ternary dye adsorption onto MnO ₂ nanoparticle-loaded activated carbon: derivative spectrophotometry and modeling. RSC Advances, 2015, 5, 72300-72320.	3.6	129
42	Least square-support vector (LS-SVM) method for modeling of methylene blue dye adsorption using copper oxide loaded on activated carbon: Kinetic and isotherm study. Journal of Industrial and Engineering Chemistry, 2014, 20, 1641-1649.	5.8	128
43	Rosmarinus officinalis leaf extract mediated green synthesis of silver nanoparticles and investigation of its antimicrobial properties. Journal of Industrial and Engineering Chemistry, 2015, 31, 167-172.	5.8	128
44	Application of ZnO nanorods loaded on activated carbon for ultrasonic assisted dyes removal: Experimental design and derivative spectrophotometry method. Ultrasonics Sonochemistry, 2016, 33, 197-209.	8.2	127
45	Hollow porous molecularly imprinted polymer for highly selective clean-up followed by influential preconcentration of ultra-trace glibenclamide from bio-fluid. Journal of Chromatography A, 2017, 1520, 65-74.	3.7	127
46	Isotherms and kinetic study of ultrasound-assisted adsorption of malachite green and Pb2+ ions from aqueous samples by copper sulfide nanorods loaded on activated carbon: Experimental design optimization. Ultrasonics Sonochemistry, 2018, 40, 373-382.	8.2	127
47	Experimental design and modeling of ultrasound assisted simultaneous adsorption of cationic dyes onto ZnS: Mn-NPs-AC from binary mixture. Ultrasonics Sonochemistry, 2016, 33, 77-89.	8.2	125
48	Application of artificial neural network and response surface methodology for the removal of crystal violet by zinc oxide nanorods loaded on activate carbon: kinetics and equilibrium study. Journal of the Taiwan Institute of Chemical Engineers, 2016, 59, 210-220.	5.3	122
49	Preparation of nanomaterials for the ultrasound-enhanced removal of Pb2+ ions and malachite green dye: Chemometric optimization and modeling. Ultrasonics Sonochemistry, 2017, 34, 677-691.	8.2	121
50	Flame atomic absorption spectrometric determination of zinc, nickel, iron and lead in different matrixes after solid phase extraction on sodium dodecyl sulfate (SDS)-coated alumina as their bis (2-hydroxyacetophenone)-1, 3-propanediimine chelates. Journal of Hazardous Materials, 2009, 166, 1441-1448.	12.4	119
51	Flame atomic absorption spectrometric determination of trace amounts of heavy metal ions after solid phase extraction using modified sodium dodecyl sulfate coated on alumina. Journal of Hazardous Materials, 2008, 155, 121-127.	12.4	118
52	A hybrid artificial neural network and particle swarm optimization for prediction of removal of hazardous dye brilliant green from aqueous solution using zinc sulfide nanoparticle loaded on activated carbon. Spectrochimica Acta - Part A: Molecular and Biomolecular Spectroscopy, 2015, 137, 1004-1015.	3.9	118
53	Performance of CuS nanoparticle loaded on activated carbon in the adsorption of methylene blue and bromophenol blue dyes in binary aqueous solutions: Using ultrasound power and optimization by central composite design. Journal of Molecular Liquids, 2016, 219, 667-676.	4.9	118
54	Flame atomic absorption spectrometric determination of copper, zinc and manganese after solid-phase extraction using 2,6-dichlorophenyl-3,3-bis(indolyl)methane loaded on Amberlite XAD-16. Food and Chemical Toxicology, 2010, 48, 891-897.	3.6	117

#	Article	IF	CITATIONS
55	Hydrogel membranes: A review. Materials Science and Engineering C, 2020, 114, 111023.	7.3	117
56	Central composite design and genetic algorithm applied for the optimization of ultrasonic-assisted removal of malachite green by ZnO Nanorod-loaded activated carbon. Spectrochimica Acta - Part A: Molecular and Biomolecular Spectroscopy, 2016, 167, 157-164.	3.9	114
57	Response surface methodology approach for optimization of adsorption of Janus Green B from aqueous solution onto ZnO/Zn(OH)2-NP-AC: Kinetic and isotherm study. Spectrochimica Acta - Part A: Molecular and Biomolecular Spectroscopy, 2016, 152, 233-240.	3.9	114
58	Water compatible molecularly imprinted nanoparticles as a restricted access material for extraction of hippuric acid, a biological indicator of toluene exposure, from human urine. Mikrochimica Acta, 2017, 184, 879-887.	5.0	113
59	Fe3O4-FeMoS4: Promise magnetite LDH-based adsorbent for simultaneous removal of Pb (II), Cd (II), and Cu (II) heavy metal ions. Journal of Hazardous Materials, 2021, 410, 124560.	12.4	113
60	Sonochemical assisted hydrothermal synthesis of ZnO: Cr nanoparticles loaded activated carbon for simultaneous ultrasound-assisted adsorption of ternary toxic organic dye: Derivative spectrophotometric, optimization, kinetic and isotherm study. Ultrasonics Sonochemistry, 2016, 32, 119-131.	8.2	110
61	Fabrication of water-compatible superparamagnetic molecularly imprinted biopolymer for clean separation of baclofen from bio-fluid samples: A mild and green approach. Talanta, 2018, 179, 760-768.	5.5	110
62	Ultrasound-assisted removal of Al ³⁺ ions and Alizarin red S by activated carbon engrafted with Ag nanoparticles: central composite design and genetic algorithm optimization. RSC Advances, 2015, 5, 59522-59532.	3.6	109
63	Ultrasound assisted adsorption of malachite green dye onto ZnS:Cu-NP-AC: Equilibrium isotherms and kinetic studies – Response surface optimization. Separation and Purification Technology, 2015, 156, 780-788.	7.9	108
64	Application of hydrophobic deep eutectic solvent as the carrier for ferrofluid: A novel strategy for pre-concentration and determination of mefenamic acid in human urine samples by high performance liquid chromatography under experimental design optimization. Talanta, 2019, 202, 526-530.	5.5	108
65	Design and construction of nanoscale material for ultrasonic assisted adsorption of dyes: Application of derivative spectrophotometry and experimental design methodology. Ultrasonics Sonochemistry, 2017, 35, 112-123.	8.2	107
66	Ultrasound assisted combined molecularly imprinted polymer for selective extraction of nicotinamide in human urine and milk samples: Spectrophotometric determination and optimization study. Ultrasonics Sonochemistry, 2017, 34, 640-650.	8.2	106
67	Artificial neural network-genetic algorithm based optimization for the adsorption of methylene blue and brilliant green from aqueous solution by graphite oxide nanoparticle. Spectrochimica Acta - Part A: Molecular and Biomolecular Spectroscopy, 2014, 125, 264-277.	3.9	105
68	Adsorption of copper (II) using modified activated carbon prepared from Pomegranate wood: Optimization by bee algorithm and response surface methodology. Journal of Molecular Liquids, 2015, 206, 195-206.	4.9	103
69	BiPO ₄ /Bi ₂ S ₃ -HKUST-1-MOF as a novel blue light-driven photocatalyst for simultaneous degradation of toluidine blue and auramine-O dyes in a new rotating packed bed reactor: optimization and comparison to a conventional reactor. RSC Advances, 2016, 6, 63667-63680.	3.6	103
70	Simultaneous removal of dyes onto nanowires adsorbent use of ultrasound assisted adsorption to clean waste water: Chemometrics for modeling and optimization, multicomponent adsorption and kinetic study. Chemical Engineering Research and Design, 2017, 124, 222-237.	5.6	103
71	Ultrasonic-assisted magnetic solid phase extraction of morphine in urine samples by new imprinted polymer-supported on MWCNT-Fe3O4-NPs: Central composite design optimization. Ultrasonics Sonochemistry, 2016, 33, 240-248.	8.2	100
72	Ultrasound wave assisted adsorption of congo red using gold-magnetic nanocomposite loaded on activated carbon: Optimization of process parameters. Ultrasonics Sonochemistry, 2018, 46, 99-105.	8.2	100

#	Article	IF	CITATIONS
73	Application of least squares support vector regression and linear multiple regression for modeling removal of methyl orange onto tin oxide nanoparticles loaded on activated carbon and activated carbon prepared from Pistacia atlantica wood. Journal of Colloid and Interface Science, 2016, 461, 425-434.	9.4	99
74	Isotherm and kinetics study of malachite green adsorption onto copper nanowires loaded on activated carbon: Artificial neural network modeling and genetic algorithm optimization. Spectrochimica Acta - Part A: Molecular and Biomolecular Spectroscopy, 2015, 142, 135-149.	3.9	96
75	Optimization of ultrasound-assisted dispersive solid-phase microextraction based on nanoparticles followed by spectrophotometry for the simultaneous determination of dyes using experimental design. Ultrasonics Sonochemistry, 2016, 32, 407-417.	8.2	95
76	Optimization of the process parameters for the adsorption of ternary dyes by Ni doped FeO(OH)-NWs–AC using response surface methodology and an artificial neural network. RSC Advances, 2016, 6, 19768-19779.	3.6	95
77	Preparation and characterization of MWCNTs functionalized by N-(3-nitrobenzylidene)-Nâ€ ² -trimethoxysilylpropyl-ethane-1,2-diamine for the removal of aluminum(<scp>iii</scp>) ions via complexation with eriochrome cyanine R: spectrophotometric detection and optimization. RSC Advances. 2015. 5. 61060-61069.	3.6	94
78	Ag 3 PO 4 /AgBr/Ag-HKUST-1-MOF composites as novel blue LED light active photocatalyst for enhanced degradation of ternary mixture of dyes in a rotating packed bed reactor. Chemical Engineering and Processing: Process Intensification, 2017, 114, 24-38.	3.6	94
79	Synthesis of nickel sulfide nanoparticles loaded on activated carbon as a novel adsorbent for the competitive removal of Methylene blue and Safranin-O. Spectrochimica Acta - Part A: Molecular and Biomolecular Spectroscopy, 2014, 123, 402-409.	3.9	93
80	A simple ultrasensitive electrochemical sensor for simultaneous determination of gallic acid and uric acid in human urine and fruit juices based on zirconia-choline chloride-gold nanoparticles-modified carbon paste electrode. Biosensors and Bioelectronics, 2018, 114, 30-36.	10.1	93
81	Synthesis and application of in-situ molecularly imprinted silica monolithic in pipette-tip solid-phase microextraction for the separation and determination of gallic acid in orange juice samples. Journal of Chromatography B: Analytical Technologies in the Biomedical and Life Sciences, 2017, 1048, 102-110.	2.3	92
82	Local, cheep and nontoxic activated carbon as efficient adsorbent for the simultaneous removal of cadmium ions and malachite green: Optimization by surface response methodology. Journal of Industrial and Engineering Chemistry, 2015, 21, 760-767.	5.8	91
83	Modeling and optimization of simultaneous removal of ternary dyes onto copper sulfide nanoparticles loaded on activated carbon using second-derivative spectrophotometry. Journal of the Taiwan Institute of Chemical Engineers, 2016, 65, 212-224.	5.3	91
84	New ion-imprinted polymer-functionalized mesoporous SBA-15 for selective separation and preconcentration of Cr(<scp>iii</scp>) ions: modeling and optimization. RSC Advances, 2015, 5, 105789-105799.	3.6	90
85	Modeling and optimization of Hg ²⁺ ion biosorption by live yeast Yarrowia lipolytica 70562 from aqueous solutions under artificial neural network-genetic algorithm and response surface methodology: kinetic and equilibrium study. RSC Advances, 2016, 6, 54149-54161.	3.6	90
86	Study of competitive adsorption of malachite green and sunset yellow dyes on cadmium hydroxide nanowires loaded on activated carbon. Journal of Industrial and Engineering Chemistry, 2014, 20, 1085-1096.	5.8	89
87	Optimizing adsorptive removal of malachite green and methyl orange dyes from simulated wastewater by Mnâ€doped CuOâ€Nanoparticles loaded on activated carbon using CCDâ€RSM: Mechanism, regeneration, isotherm, kinetic, and thermodynamic studies. Applied Organometallic Chemistry, 2019, 33, e4768.	3.5	88
88	Multi-response optimization of ultrasound assisted competitive adsorption of dyes onto Cu (OH)2-nanoparticle loaded activated carbon: Central composite design. Ultrasonics Sonochemistry, 2017, 34, 343-353.	8.2	87
89	Cadmium hydroxide nanowire loaded on activated carbon as efficient adsorbent for removal of Bromocresol Green. Spectrochimica Acta - Part A: Molecular and Biomolecular Spectroscopy, 2012, 86, 62-68.	3.9	85
90	Rapid and high-capacity ultrasonic assisted adsorption of ternary toxic anionic dyes onto MOF-5-activated carbon: Artificial neural networks, partial least squares, desirability function and isotherm and kinetic study. Ultrasonics Sonochemistry, 2017, 37, 71-82.	8.2	85

#	Article	IF	CITATIONS
91	Cadmium telluride nanoparticles loaded on activated carbon as adsorbent for removal of sunset yellow. Spectrochimica Acta - Part A: Molecular and Biomolecular Spectroscopy, 2012, 90, 22-27.	3.9	84
92	Tin oxide nanoparticle loaded on activated carbon as new adsorbent for efficient removal of malachite green-oxalate: Non-linear kinetics and isotherm study. Journal of Molecular Liquids, 2014, 195, 212-218.	4.9	84
93	Synthesis of ZnO-nanorod-based materials for antibacterial, antifungal activities, DNA cleavage and efficient ultrasound-assisted dyes adsorption. Ecotoxicology and Environmental Safety, 2017, 142, 330-337.	6.0	84
94	Comparison of cadmium hydroxide nanowires and silver nanoparticles loaded on activated carbon as new adsorbents for efficient removal of Sunset yellow: Kinetics and equilibrium study. Spectrochimica Acta - Part A: Molecular and Biomolecular Spectroscopy, 2012, 94, 346-351.	3.9	83
95	Simultaneous removal of methylene blue and Pb ²⁺ ions using ruthenium nanoparticle-loaded activated carbon: response surface methodology. RSC Advances, 2015, 5, 83427-83435.	3.6	83
96	Principal component analysis- adaptive neuro-fuzzy inference system modeling and genetic algorithm optimization of adsorption of methylene blue by activated carbon derived from Pistacia khinjuk. Ecotoxicology and Environmental Safety, 2013, 96, 110-117.	6.0	82
97	Artificial neural network (ANN) method for modeling of sunset yellow dye adsorption using zinc oxide nanorods loaded on activated carbon: Kinetic and isotherm study. Spectrochimica Acta - Part A: Molecular and Biomolecular Spectroscopy, 2015, 134, 1-9.	3.9	82
98	Rapid adsorption of ternary dye pollutants onto copper (I) oxide nanoparticle loaded on activated carbon: Experimental optimization via response surface methodology. Journal of Environmental Chemical Engineering, 2016, 4, 1769-1779.	6.7	82
99	Trace determination of safranin O dye using ultrasound assisted dispersive solid-phase micro extraction: Artificial neural network-genetic algorithm and response surface methodology. Ultrasonics Sonochemistry, 2016, 33, 129-140.	8.2	81
100	Biosorption of Zn ²⁺ , Ni ²⁺ and Co ²⁺ from water samples onto Yarrowia lipolytica ISF7 using a response surface methodology, and analyzed by inductively coupled plasma optical emission spectrometry (ICP-OES). RSC Advances, 2016, 6, 23599-23610.	3.6	80
101	Simple and selective detection of quercetin in extracts of plants and food samples by dispersive-micro-solid phase extraction based on core–shell magnetic molecularly imprinted polymers. New Journal of Chemistry, 2018, 42, 16144-16153.	2.8	80
102	Application of experimental design and derivative spectrophotometry methods in optimization and analysis of biosorption of binary mixtures of basic dyes from aqueous solutions. Ecotoxicology and Environmental Safety, 2017, 139, 219-227.	6.0	79
103	Novel synthesis of nanocomposite for the extraction of Sildenafil Citrate (Viagra) from water and urine samples: Process screening and optimization. Ultrasonics Sonochemistry, 2017, 38, 463-472.	8.2	79
104	Ultrasonic assisted removal of methylene blue on ultrasonically synthesized zinc hydroxide nanoparticles on activated carbon prepared from wood of cherry tree: Experimental design methodology and artificial neural network. Journal of Molecular Liquids, 2017, 229, 114-124.	4.9	79
105	Comparison between dispersive liquid–liquid microextraction and ultrasound-assisted nanoparticles-dispersive solid-phase microextraction combined with microvolume spectrophotometry method for the determination of Auramine-O in water samples. RSC Advances, 2015, 5, 39084-39096.	3.6	78
106	Synthesis and application of molecularly imprinted nanoparticles combined ultrasonic assisted for highly selective solid phase extraction trace amount of celecoxib from human plasma samples using design expert (DXB) software. Ultrasonics Sonochemistry, 2016, 33, 67-76.	8.2	78
107	Synthesis and application of Ce-doped TiO2 nanoparticles loaded on activated carbon for ultrasound-assisted adsorption of Basic Red 46 dye. Ultrasonics Sonochemistry, 2019, 58, 104702.	8.2	78
108	Column packing elimination in matrix solid phase dispersion by using water compatible magnetic molecularly imprinted polymer for recognition of melamine from milk samples. Journal of Chromatography A, 2019, 1594, 13-22.	3.7	78

#	Article	IF	CITATIONS
109	Simultaneous ultrasound-assisted removal of sunset yellow and erythrosine by ZnS:Ni nanoparticles loaded on activated carbon: Optimization by central composite design. Ultrasonics Sonochemistry, 2014, 21, 1441-1450.	8.2	77
110	Simultaneous ultrasonic-assisted removal of malachite green and safranin O by copper nanowires loaded on activated carbon: central composite design optimization. RSC Advances, 2015, 5, 57021-57029.	3.6	77
111	Efficient removal of radioactive uranium from solvent phase using AgOH–MWCNTs nanoparticles: Kinetic and thermodynamic study. Chemical Engineering Journal, 2015, 273, 296-306.	12.7	77
112	Magnetic Cu: CuO-GO nanocomposite for efficient dispersive micro-solid phase extraction of polycyclic aromatic hydrocarbons from vegetable, fruit, and environmental water samples by liquid chromatographic determination. Talanta, 2020, 218, 121131.	5.5	77
113	Oxidized multiwalled carbon nanotubes as efficient adsorbent for bromothymol blue. Toxicological and Environmental Chemistry, 2012, 94, 873-883.	1.2	76
114	Cu@SnS/SnO2 nanoparticles as novel sorbent for dispersive micro solid phase extraction of atorvastatin in human plasma and urine samples by high-performance liquid chromatography with UV detection: Application of central composite design (CCD). Ultrasonics Sonochemistry, 2017, 36, 42-49.	8.2	76
115	Synthesis of Fe3O4@CuS@Ni2P-CNTs magnetic nanocomposite for sonochemical-assisted sorption and pre-concentration of trace Allura Red from aqueous samples prior to HPLC-UV detection: CCD-RSM design. Ultrasonics Sonochemistry, 2018, 44, 240-250.	8.2	76
116	Photo-Sensitive Pb5S2I6 crystal incorporated polydopamine biointerface coated on nanoporous TiO2 as an efficient signal-on photoelectrochemical bioassay for ultrasensitive detection of Cr(VI) ions. Biosensors and Bioelectronics, 2019, 132, 105-114.	10.1	76
117	L-phenylalanine-imprinted polydopamine-coated CdS/CdSe n-n type II heterojunction as an ultrasensitive photoelectrochemical biosensor for the PKU monitoring. Biosensors and Bioelectronics, 2020, 165, 112346.	10.1	76
118	Synthesis and characterization of ZnS:Ni-NPs loaded on AC derived from apple tree wood and their applicability for the ultrasound assisted comparative adsorption of cationic dyes based on the experimental design. Ultrasonics Sonochemistry, 2017, 38, 371-380.	8.2	75
119	Biosorption of malachite green by novel biosorbent Yarrowia lipolytica isf7: Application of response surface methodology. Journal of Molecular Liquids, 2016, 214, 249-258.	4.9	74
120	Improved adsorption performance of nanostructured composite by ultrasonic wave: Optimization through response surface methodology, isotherm and kinetic studies. Ultrasonics Sonochemistry, 2017, 37, 94-105.	8.2	74
121	H2S adsorption onto Cu-Zn–Ni nanoparticles loaded activated carbon and Ni-Co nanoparticles loaded γ-Al2O3: Optimization and adsorption isotherms. Journal of Colloid and Interface Science, 2017, 490, 553-561.	9.4	74
122	UiO-66(Ti)-Fe3O4-WO3 photocatalyst for efficient ammonia degradation from wastewater into continuous flow-loop thin film slurry flat-plate photoreactor. Journal of Hazardous Materials, 2020, 393, 122360.	12.4	74
123	Comparison of Activated Carbon and Multiwalled Carbon Nanotubes for Efficient Removal of Eriochrome Cyanine R (ECR): Kinetic, Isotherm, and Thermodynamic Study of the Removal Process. Journal of Chemical & Engineering Data, 2011, 56, 3227-3235.	1.9	73
124	Novel nanorose-like Ce(<scp>iii</scp>)-doped and undoped Cu(<scp>ii</scp>)–biphenyl-4,4-dicarboxylic acid (Cu(<scp>ii</scp>)–BPDCA) MOSs as visible light photocatalysts: synthesis, characterization, photodegradation of toxic dyes and optimization. Physical Chemistry Chemical Physics, 2016, 18, 11278-11287.	2.8	73
125	Cu- and S- @SnO2 nanoparticles loaded on activated carbon for efficient ultrasound assisted dispersive ŵSPE-spectrophotometric detection of quercetin in Nasturtium officinale extract and fruit juice samples: CCD-RSM design. Ultrasonics Sonochemistry, 2018, 47, 1-9.	8.2	73
126	ZnS:Cu nanoparticles loaded on activated carbon as novel adsorbent for kinetic, thermodynamic and isotherm studies of Reactive Orange 12 and Direct yellow 12 adsorption. Spectrochimica Acta - Part A: Molecular and Biomolecular Spectroscopy, 2013, 114, 687-694.	3.9	72

MEHRORANG GHAEDI

#	Article	IF	CITATIONS
127	Random forest model for the ultrasonic-assisted removal of chrysoidine G by copper sulfide nanoparticles loaded on activated carbon; response surface methodology approach. RSC Advances, 2015, 5, 59335-59343.	3.6	72
128	Titanium oxide nanoparticles loaded onto activated carbon prepared from bio-waste watermelon rind for the efficient ultrasonic-assisted adsorption of congo red and phenol red dyes from wastewaters. Polyhedron, 2019, 173, 114105.	2.2	72
129	Optimization and modeling of preconcentration and determination of dyes based on ultrasound assisted-dispersive liquid–liquid microextraction coupled with derivative spectrophotometry. Ultrasonics Sonochemistry, 2017, 34, 27-36.	8.2	71
130	Synthesis and characterization of ZnO-nanorods loaded onto activated carbon and its application for efficient solid phase extraction and determination of BG from water samples by micro-volume spectrophotometry. New Journal of Chemistry, 2015, 39, 9407-9414.	2.8	70
131	Artificial neural network and particle swarm optimization for removal of methyl orange by gold nanoparticles loaded on activated carbon and Tamarisk. Spectrochimica Acta - Part A: Molecular and Biomolecular Spectroscopy, 2014, 132, 639-654.	3.9	69
132	Optimization of process parameters for determination of trace Hazardous dyes from industrial wastewaters based on nanostructures materials under ultrasound energy. Ultrasonics Sonochemistry, 2018, 40, 238-248.	8.2	69
133	Activated carbon and multiwalled carbon nanotubes as efficient adsorbents for removal of arsenazo(ΙΙΙ) and methyl red from waste water. Toxicological and Environmental Chemistry, 2011, 93, 438-449.	1.2	68
134	Ultrasound assisted extraction of Maxilon Red GRL dye from water samples using cobalt ferrite nanoparticles loaded on activated carbon as sorbent: Optimization and modeling. Ultrasonics Sonochemistry, 2017, 38, 672-680.	8.2	68
135	Preparation and characterization of an ACa€"Fe ₃ O ₄ a€"Au hybrid for the simultaneous removal of Cd ²⁺ , Pb ²⁺ , Cr ³⁺ and Ni ²⁺ ions from aqueous solution via complexation with 2-((2,4-dichloro-benzylidene)-amino)-benzenethiol: Taguchi optimization. RSC Advances, 2016, 6,	3.6	67
136	Optimization and characterization of ultrasound assisted preparation of curcumin-loaded solid lipid nanoparticles: Application of central composite design, thermal analysis and X-ray diffraction techniques. Ultrasonics Sonochemistry, 2017, 38, 271-280.	8.2	67
137	Nano-sized FeO@SiO-molecular imprinted polymer as a sorbent for dispersive solid-phase microextraction of melatonin in the methanolic extract of , biological, and water samples. Talanta, 2021, 221, 121620.	5.5	67
138	Synthesis of lab-in-a-pipette-tip extraction using hydrophilic nano-sized dummy molecularly imprinted polymer for purification and analysis of prednisolone. Journal of Colloid and Interface Science, 2016, 480, 232-239.	9.4	66
139	HKUST-1-MOF–BiVO ₄ hybrid as a new sonophotocatalyst for simultaneous degradation of disulfine blue and rose bengal dyes: optimization and statistical modelling. RSC Advances, 2016, 6, 61516-61527.	3.6	66
140	A ferrofluidic hydrophobic deep eutectic solvent for the extraction of doxycycline from urine, blood plasma and milk samples prior to its determination by high-performance liquid chromatography-ultraviolet. Journal of Chromatography A, 2020, 1613, 460695.	3.7	66
141	Removal of methylene blue from aqueous solution by wood millet carbon optimization using response surface methodology. Spectrochimica Acta - Part A: Molecular and Biomolecular Spectroscopy, 2015, 136, 141-148.	3.9	65
142	Synthesis and characterization of Au-NPs supported on carbon nanotubes: Application for the ultrasound assisted removal of radioactive UO22+ ions following complexation with Arsenazo III: Spectrophotometric detection, optimization, isotherm and kinetic study. Journal of Colloid and Interface Science, 2017, 504, 68-77.	9.4	65
143	Novel visible light-driven Cu-based MOFs/Ag ₂ O composite photocatalysts with enhanced photocatalytic activity toward the degradation of orange G: their photocatalytic mechanism and optimization study. New Journal of Chemistry, 2018, 42, 9720-9734.	2.8	65
144	Comparative studies on removal of Erythrosine using ZnS and AgOH nanoparticles loaded on activated carbon as adsorbents: Kinetic and isotherm studies of adsorption. Spectrochimica Acta - Part A: Molecular and Biomolecular Spectroscopy, 2015, 138, 176-186.	3.9	64

#	Article	IF	CITATIONS
145	Comparison of nickel doped Zinc Sulfide and/or palladium nanoparticle loaded on activated carbon as efficient adsorbents for kinetic and equilibrium study of removal of Congo Red dye. Spectrochimica Acta - Part A: Molecular and Biomolecular Spectroscopy, 2015, 136, 1441-1449.	3.9	63
146	Adsorption of semisoft pollutants onto Bi 2 S 3 /Ag 2 S-AC under the influence of ultrasonic waves as external filed. Journal of Industrial and Engineering Chemistry, 2018, 60, 390-400.	5.8	62
147	Potentiality of white-rot fungi in biosorption of nickel and cadmium: Modeling optimization and kinetics study. Chemosphere, 2019, 216, 124-130.	8.2	62
148	Application of random forest, radial basis function neural networks and central composite design for modeling and/or optimization of the ultrasonic assisted adsorption of brilliant green on ZnS-NP-AC. Journal of Colloid and Interface Science, 2017, 505, 278-292.	9.4	61
149	Magnetic based nanocomposite sorbent combination with ultrasound assisted for solid-phase microextraction of Azure II in water samples prior to its determination spectrophotometric. Journal of Colloid and Interface Science, 2018, 513, 240-250.	9.4	60
150	Enhanced visible light-active CeO ₂ /CuO/Ag ₂ CrO ₄ ternary heterostructures based on CeO ₂ /CuO nanofiber heterojunctions for the simultaneous degradation of a binary mixture of dyes. New Journal of Chemistry, 2020, 44, 5033-5048.	2.8	60
151	Flame atomic absorption spectrometric (FAAS) determination of copper, iron and zinc in food samples after solid-phase extraction on Schiff base-modified duolite XAD 761. Materials Science and Engineering C, 2013, 33, 2338-2344.	7.3	59
152	Preparation of a new chromium(III) selective electrode based on 1-[(2-hydroxy ethyl) amino]-4-methyl-9H-thioxanthen-9-one as a neutral carrier. Journal of Hazardous Materials, 2010, 178, 157-163.	12.4	58
153	Experimental design for simultaneous analysis of malachite green and methylene blue; derivative spectrophotometry and principal component-artificial neural network. RSC Advances, 2015, 5, 38939-38947.	3.6	58
154	Bi ₂ WO ₆ /Ag ₃ PO ₄ –Ag Z-scheme heterojunction as a new plasmonic visible-light-driven photocatalyst: performance evaluation and mechanism study. New Journal of Chemistry, 2019, 43, 1275-1284.	2.8	58
155	Silica chemically bonded N-propyl kriptofix 21 and 22 with immobilized palladium nanoparticles for solid phase extraction and preconcentration of some metal ions. Materials Science and Engineering C, 2013, 33, 3180-3189.	7.3	57
156	Simultaneous removing of Pb2+ ions and alizarin red S dye after their complexation by ultrasonic waves coupled adsorption process: Spectrophotometry detection and optimization study. Ultrasonics Sonochemistry, 2017, 35, 51-60.	8.2	57
157	Oxidized multiwalled carbon nanotubes for the removal of methyl red (MR): kinetics and equilibrium study. Desalination and Water Treatment, 2012, 49, 317-325.	1.0	56
158	Adaptive neuro-fuzzy inference system model for adsorption of 1,3,4-thiadiazole-2,5-dithiol onto gold nanoparticales-activated carbon. Spectrochimica Acta - Part A: Molecular and Biomolecular Spectroscopy, 2014, 131, 606-614.	3.9	56
159	Artificial neural network-genetic algorithm based optimization for the adsorption of phenol red (PR) onto gold and titanium dioxide nanoparticles loaded on activated carbon. Journal of Industrial and Engineering Chemistry, 2015, 21, 587-598.	5.8	56
160	Comparison between dispersive solid-phase and dispersive liquid–liquid microextraction combined with spectrophotometric determination of malachite green in water samples based on ultrasound-assisted and preconcentration under multi-variable experimental design optimization. Ultrasonics Sonochemistry, 2017, 39, 374-383.	8.2	56
161	Artificial neural network – Imperialist competitive algorithm based optimization for removal of sunset yellow using Zn(OH)2 nanoparticles-activated carbon. Journal of Industrial and Engineering Chemistry, 2014, 20, 4332-4343.	5.8	55
162	Ultrasound-assisted adsorption of Sunset Yellow CFC dye onto Cu doped ZnS nanoparticles loaded on activated carbon using response surface methodology based on central composite design. Journal of Molecular Liquids, 2016, 219, 332-340.	4.9	55

#	Article	IF	CITATIONS
163	Chemically bonded multiwalled carbon nanotubes as efficient material for solid phase extraction of some metal ions in food samples. International Journal of Environmental Analytical Chemistry, 2013, 93, 528-542.	3.3	54
164	Chitosan extraction from lobster shells and its grafted with functionalized MWCNT for simultaneous removal of Pb 2+ ions and eriochrome cyanine R dye after their complexation. International Journal of Biological Macromolecules, 2017, 102, 181-191.	7.5	54
165	Synthesis of regenerable Zn(OH) ₂ nanoparticle-loaded activated carbon for the ultrasound-assisted removal of malachite green: optimization, isotherm and kinetics. RSC Advances, 2015, 5, 79119-79128.	3.6	53
166	Simultaneous removal of Cd(II), Ni(II), Pb(II) and Cu(II) ions via their complexation with HBANSA based on a combined ultrasound-assisted and cloud point adsorption method using CSG-BiPO 4 /FePO 4 as novel adsorbent: FAAS detection and optimization process. Journal of Colloid and Interface Science, 2017, 500, 241-252.	9.4	53
167	Fixed-bed column performances of azure-II and auramine-O adsorption by Pinus eldarica stalks activated carbon and its composite with zno nanoparticles: Optimization by response surface methodology based on central composite design. Journal of Colloid and Interface Science, 2017, 507, 172-189.	9.4	53
168	Design of a new technique based on combination of ultrasound waves via magnetite solid phase and cloud point microextraction for determination of Cr(III) ions. Ultrasonics Sonochemistry, 2017, 39, 798-809.	8.2	52
169	Sensitized spectrophotometric determination of Cr(III) ion for speciation of chromium ion in surfactant media using α-benzoin oxime. Spectrochimica Acta - Part A: Molecular and Biomolecular Spectroscopy, 2006, 63, 182-188.	3.9	51
170	Selective and sensitized spectrophotometric determination of trace amounts of Ni(II) ion using α-benzyl dioxime in surfactant media. Spectrochimica Acta - Part A: Molecular and Biomolecular Spectroscopy, 2007, 66, 295-301.	3.9	51
171	Application of modificated magnetic nanomaterial for optimization of ultrasound-enhanced removal of Pb2+ ions from aqueous solution under experimental design: Investigation of kinetic and isotherm. Ultrasonics Sonochemistry, 2017, 36, 409-419.	8.2	50
172	Multi-responses optimization of simultaneous biosorption of cationic dyes by live yeast Yarrowia lipolytica 70562 from binary solution: Application of first order derivative spectrophotometry. Ecotoxicology and Environmental Safety, 2017, 139, 158-164.	6.0	49
173	Nanocomposites: Synthesis, characterization and its application to removal azo dyes using ultrasonic assisted method: Modeling and optimization. Ultrasonics Sonochemistry, 2017, 38, 530-543.	8.2	49
174	Application of Molecularly Imprinted Biomembrane for Advancement of Matrix Solid-Phase Dispersion for Clean Enrichment of Parabens from Powder Sunscreen Samples: Optimization of Chromatographic Conditions and Green Approach. ACS Omega, 2019, 4, 3839-3849.	3.5	49
175	Preconcentration and separation of trace amount of heavy metal ions on bis(2-hydroxy) Tj ETQq1 1 0.784314 rgB 1408-1414.	T /Overloo 12.4	ck 10 Tf 50 2 48
176	Equilibrium, kinetic and thermodynamic study of removal of reactive orange 12 on platinum nanoparticle loaded on activated carbon as novel adsorbent. Korean Journal of Chemical Engineering, 2011, 28, 2255-2261.	2.7	48
177	Solid phase extraction and removal of brilliant green dye on zinc oxide nanoparticles loaded on activated carbon: New kinetic model and thermodynamic evaluation. Journal of Industrial and Engineering Chemistry, 2014, 20, 1444-1452.	5.8	48
178	Green preparation of dual-template chitosan-based magnetic water-compatible molecularly imprinted biopolymer. Carbohydrate Polymers, 2020, 236, 116102.	10.2	48
179	Modification of Gold Nanoparticle Loaded on Activated Carbon with Bis(4-methoxysalicylaldehyde)-1,2-Phenylenediamine as New Sorbent for Enrichment of Some Metal Ions. Biological Trace Element Research, 2012, 145, 109-117.	3.5	47
180	Nano-sized molecularly imprinted polymer for selective ultrasound-assisted microextraction of pesticide Carbaryl from water samples: Spectrophotometric determination. Journal of Colloid and Interface Science, 2017, 498, 313-322.	9.4	47

#	Article	IF	CITATIONS
181	Electrospinning preparation of NiO/ZnO composite nanofibers for photodegradation of binary mixture of rhodamine B and methylene blue in aqueous solution: Central composite optimization. Applied Organometallic Chemistry, 2018, 32, e4335.	3.5	47
182	Ultrasound-accelerated synthesis of gold nanoparticles modified choline chloride functionalized graphene oxide as a novel sensitive bioelectrochemical sensor: Optimized meloxicam detection using CCD-RSM design and application for human plasma sample. Ultrasonics Sonochemistry, 2018, 42, 776-786.	8.2	47
183	Synthesis of chitosan based molecularly imprinted polymer for pipette-tip solid phase extraction of Rhodamine B from chili powder samples. International Journal of Biological Macromolecules, 2019, 139, 40-48.	7.5	47
184	Modeling and optimization of ultrasound-assisted high performance adsorption of Basic Fuchsin by starch-capped zinc selenide nanoparticles/AC as a novel composite using response surface methodology. International Journal of Biological Macromolecules, 2020, 152, 913-921.	7.5	47
185	Simultaneous Preconcentration of Copper, Nickel, Cobalt and Lead Ions Prior to Their Flame Atomic Absorption Spectrometric Determination. Annali Di Chimica, 2007, 97, 277-285.	0.6	46
186	Comparison of Activated Carbon, Multiwalled Carbon Nanotubes, and Cadmium Hydroxide Nanowire Loaded on Activated Carbon as Adsorbents for Kinetic and Equilibrium Study of Removal of Safranine O. Spectroscopy Letters, 2012, 45, 500-510.	1.0	46
187	Magnetic molecularly imprinted polymer for the efficient and selective preconcentration of diazinon before its determination by high-performance liquid chromatography. Journal of Separation Science, 2015, 38, 2797-2803.	2.5	46
188	Preparation of Iodide Selective Carbon Paste Electrode with Modified Carbon Nanotubes by Potentiometric Method and Effect of CuSâ€NPs on Its Response. Electroanalysis, 2015, 27, 1516-1522.	2.9	46
189	Ultrasound assisted microextraction-nano material solid phase dispersion for extraction and determination of thymol and carvacrol in pharmaceutical samples: Experimental design methodology. Journal of Chromatography B: Analytical Technologies in the Biomedical and Life Sciences, 2015, 975, 34-39.	2.3	46
190	Ultrasonically assisted removal of Congo Red, Phloxine B and Fast green FCF in ternary mixture using novel nanocomposite following their simultaneous analysis by derivative spectrophotometry. Ultrasonics Sonochemistry, 2017, 37, 452-463.	8.2	46
191	Mild synthesis of a Zn(II) metal organic polymer and its hybrid with activated carbon: Application as antibacterial agent and in water treatment by using sonochemistry: Optimization, kinetic and isotherm study. Ultrasonics Sonochemistry, 2018, 41, 389-396.	8.2	46
192	Nanofibers based quaternary CeO2/Co3O4/Ag/Ag3PO4 S-scheme heterojunction photocatalyst with enhanced degradation of organic dyes. Materials Research Bulletin, 2022, 147, 111629.	5.2	46
193	Development of efficient method for preconcentration and determination of copper, nickel, zinc and iron ions in environmental samples by combination of cloud point extraction and flame atomic absorption spectrometry. Open Chemistry, 2009, 7, 148-154.	1.9	45
194	Cloud Point Extraction of Copper, Zinc, Iron and Nickel in Biological and Environmental Samples by Flame Atomic Absorption Spectrometry. Separation Science and Technology, 2009, 44, 773-786.	2.5	45
195	A new electrochemical sensor for simultaneous determination of arbutin and vitamin C based on hydroxyapatite-ZnO-Pd nanoparticles modified carbon paste electrode. Biosensors and Bioelectronics, 2019, 141, 111474.	10.1	45
196	Sonophotocatalytic treatment of rhodamine B using visible-light-driven CeO2/Ag2CrO4 composite in a batch mode based on ribbon-like CeO2 nanofibers via electrospinning. Environmental Science and Pollution Research, 2019, 26, 8050-8068.	5.3	45
197	Visible light-induced photo-degradation of methylene blue by n–p heterojunction CeO2/CuS composite based on ribbon-like CeO2 nanofibers via electrospinning. Polyhedron, 2019, 170, 160-171.	2.2	45
198	Solid phase extraction on multiwalled carbon nanotubes and flame atomic absorption spectrometry combination for determination of some metal ions in environmental and food samples. Toxicological and Environmental Chemistry, 2011, 93, 873-885.	1.2	44

#	Article	IF	CITATIONS
199	Application of optimized dispersive liquid–liquid microextraction for determination of melatonin by HPLC–UV in plasma samples. Journal of Chromatography B: Analytical Technologies in the Biomedical and Life Sciences, 2014, 960, 1-7.	2.3	44
200	Comparison of ultrasonic with stirrer performance for removal of sunset yellow (SY) by activated carbon prepared from wood of orange tree: Artificial neural network modeling. Spectrochimica Acta - Part A: Molecular and Biomolecular Spectroscopy, 2015, 138, 789-799.	3.9	43
201	Electrochemical synthesis and efficient photocatalytic degradation of azo dye alizarin yellow R by Cu/CuO nanorods under visible LED light irradiation using experimental design methodology. Polyhedron, 2019, 158, 506-514.	2.2	43
202	Congo red removal using oxidized multiwalled carbon nanotubes: kinetic and isotherm study. Desalination and Water Treatment, 2015, 53, 844-852.	1.0	42
203	MOF-5(Zn)-Fe 2 O 4 nanocomposite based magnetic solid-phase microextraction followed by HPLC-UV for efficient enrichment of colchicine in root of colchicium extracts and plasma samples. Journal of Chromatography B: Analytical Technologies in the Biomedical and Life Sciences, 2017, 1067, 45-52.	2.3	42
204	Use of metal composite MOFâ€5â€Ag ₂ Oâ€NPs as an adsorbent for the removal of Auramine O dye under ultrasound energy conditions. Applied Organometallic Chemistry, 2018, 32, e4007.	3.5	42
205	Application of Response Surface Methodology and Dispersive Liquid–Liquid Microextraction by Microvolume Spectrophotometry Method for Rapid Determination of Curcumin in Water, Wastewater, and Food Samples. Food Analytical Methods, 2016, 9, 1274-1283.	2.6	41
206	Synthesis of nanocomposites of iron oxide/gold (Fe3O4/Au) loaded on activated carbon and their application in water treatment by using sonochemistry: Optimization study. Ultrasonics Sonochemistry, 2018, 41, 279-287.	8.2	41
207	Exploration of the adsorption capability by doping Pb@ZnFe2O4 nanocomposites (NCs) for decontamination of dye from textile wastewater. Heliyon, 2019, 5, e02412.	3.2	40
208	Solid phase extraction of antidepressant drugs amitriptyline and nortriptyline from plasma samples using core-shell nanoparticles of the type Fe3O4@ZrO2@N- cetylpyridinium, and their subsequent determination by HPLC with UV detection. Mikrochimica Acta, 2015, 182, 1893-1902.	5.0	39
209	Optimization of combined ultrasonic assisted/tin sulfide nanoparticle loaded on activated carbon removal of erythrosine by response surface methodology. Journal of Industrial and Engineering Chemistry, 2015, 21, 459-469.	5.8	39
210	Sonochemical-solvothermal synthesis of guanine embedded copper based metal-organic framework (MOF) and its effect on oprD gene expression in clinical and standard strains of Pseudomonas aeruginosa. Ultrasonics Sonochemistry, 2018, 42, 237-243.	8.2	39
211	A Bi ₂ WO ₆ /Ag ₂ S/ZnS <i>Z</i> scheme heterojunction photocatalyst with enhanced visible-light photoactivity towards the degradation of multiple dye pollutants. RSC Advances, 2019, 9, 30100-30111.	3.6	39
212	Removal of paraquat from aqueous solutions by a bentonite modified zero-valent iron adsorbent. New Journal of Chemistry, 2020, 44, 13368-13376.	2.8	39
213	Highly selective magnetic dual template molecularly imprinted polymer for simultaneous enrichment of sulfadiazine and sulfathiazole from milk samples based on syringe–to–syringe magnetic solid–phase microextraction. Talanta, 2021, 232, 122449.	5.5	39
214	Synthesis, characterization, crystal structures, and solution studies of Ni(II), Cu(II) and Zn(II) complexes obtained from pyridine-2,6-dicarboxylic acid and 2,9-Dimethyl-1,10-Phenanthroline. Journal of the Iranian Chemical Society, 2009, 6, 55-70.	2.2	38
215	Equilibrium, Thermodynamic, and Kinetic Studies on Lead (II) Biosorption from Aqueous Solution by <i>Saccharomyces cerevisiae</i> Biomass. Clean - Soil, Air, Water, 2010, 38, 877-885.	1.1	37
216	Comparison of the efficiency of Cu and silver nanoparticle loaded on supports for the removal of Eosin Y from aqueous solution: Kinetic and isotherm study. Spectrochimica Acta - Part A: Molecular and Biomolecular Spectroscopy, 2014, 123, 467-472.	3.9	37

#	Article	IF	CITATIONS
217	A novel polyvinyl chloride-membrane optical sensor for the determination of Cu2+ ion based on synthesized (N′1E,N′2E)-N′1,N′2-bis(pyridine-2-ylmethylene)oxalohydrazide: Experimental design and optimization. Spectrochimica Acta - Part A: Molecular and Biomolecular Spectroscopy, 2015, 138, 878-884.	3.9	37
218	A hybrid model of support vector regression with genetic algorithm for forecasting adsorption of malachite green onto multi-walled carbon nanotubes: central composite design optimization. Physical Chemistry Chemical Physics, 2016, 18, 13310-13321.	2.8	37
219	Fabrication of polyethyleneimine modified cobalt ferrite as a new magnetic sorbent for the micro-solid phase extraction of tartrazine from food and water samples. Journal of Colloid and Interface Science, 2018, 531, 343-351.	9.4	37
220	Application of response surface methodology for determination of methyl red in water samples by spectrophotometry method. Spectrochimica Acta - Part A: Molecular and Biomolecular Spectroscopy, 2014, 133, 87-92.	3.9	36
221	Removal of methylene blue by silver nanoparticles loaded on activated carbon by an ultrasound-assisted device: optimization by experimental design methodology. Research on Chemical Intermediates, 2018, 44, 2929-2950.	2.7	36
222	A simple approach for the sonochemical loading of Au, Ag and Pd nanoparticle on functionalized MWCNT and subsequent dispersion studies for removal of organic dyes: Artificial neural network and response surface methodology studies. Ultrasonics Sonochemistry, 2018, 42, 422-433.	8.2	36
223	Highly selective MXene/V2O5/CuWO4-based ultra-sensitive room temperature ammonia sensor. Journal of Hazardous Materials, 2021, 416, 126196.	12.4	36
224	A solid phase extraction procedure for Fe3+, Cu2+ and Zn2+ ions on 2-phenyl-1H-benzo[d] imidazole loaded on Triton X-100-coated polyvinyl chloride. Journal of Hazardous Materials, 2008, 158, 131-136.	12.4	35
225	Application of experimental design for removal of sunset yellow by copper sulfide nanoparticles loaded on activated carbon. Journal of Industrial and Engineering Chemistry, 2014, 20, 2663-2670.	5.8	35
226	A random forest approach for predicting the removal of Congo red from aqueous solutions by adsorption onto tin sulfide nanoparticles loaded on activated carbon. Desalination and Water Treatment, 2016, 57, 9272-9285.	1.0	35
227	Preparation and characterization of monoliths HKUST-1 MOF <i>via</i> straightforward conversion of Cu(OH) ₂ -based monoliths and its application for wastewater treatment: artificial neural network and central composite design modeling. New Journal of Chemistry, 2018, 42, 10327-10336.	2.8	35
228	Molecular Imprinted Poly(2,5-benzimidazole)-Modified VO ₂ –CuWO ₄ Homotype Heterojunction for Photoelectrochemical Dopamine Sensing. Analytical Chemistry, 2022, 94, 6781-6790.	6.5	35
229	Optimisation of ultrasound-assisted reverse micelles dispersive liquid–liquid micro-extraction by Box–Behnken design for determination of acetoin in butter followed by high performance liquid chromatography. Food Chemistry, 2014, 161, 120-126.	8.2	34
230	Ultrasonic assisted removal of sunset yellow from aqueous solution by zinc hydroxide nanoparticle loaded activated carbon: Optimized experimental design. Materials Science and Engineering C, 2015, 52, 82-89.	7.3	34
231	The headspace solid-phase microextraction of polycyclic aromatic hydrocarbons in environmental water samples using silica fiber modified by self assembled gold nanoparticles. Analytical Methods, 2015, 7, 8086-8093.	2.7	33
232	Iodide-Selective Electrodes Based on Bis[N(2-methyl-phenyl) 4-Nitro-thiobenzamidato]mercury(II) and Bis[N-phenyl 3,5-Dinitro-thiobenzamidato]mercury(II) Carriers. Electroanalysis, 2005, 17, 1746-1754.	2.9	32
233	Application of Cloud Point Extraction for Copper, Nickel, Zinc and Iron Ions in Environmental Samples. Journal of the Chinese Chemical Society, 2009, 56, 981-986.	1.4	32
234	Zinc oxide nanorodâ€loaded activated carbon for ultrasoundâ€assisted adsorption of safranin O: Central composite design and genetic algorithm optimization. Applied Organometallic Chemistry, 2018, 32, e4099.	3.5	32

#	Article	IF	CITATIONS
235	Natural Source-Based Graphene as Sensitising Agents for Air Quality Monitoring. Scientific Reports, 2019, 9, 3798.	3.3	32
236	Synthesis and characterization of zinc sulfide nanoparticles loaded on activated carbon for the removal of methylene blue. Environmental Progress and Sustainable Energy, 2013, 32, 535-542.	2.3	31
237	Simultaneous determination of cationic dyes in water samples with dispersive liquid–liquid microextraction followed by spectrophotometry: experimental design methodology. New Journal of Chemistry, 2016, 40, 4793-4802.	2.8	31
238	Statistical optimization and modeling approach for azo dye decolorization: Combined effects of ultrasound waves and nanomaterialâ€based adsorbent. Applied Organometallic Chemistry, 2018, 32, e4205.	3.5	30
239	Preparation of hollow porous molecularly imprinted and aluminum(III) doped silica nanospheres for extraction of the drugs valsartan and losartan prior to their quantitation by HPLC. Mikrochimica Acta, 2019, 186, 702.	5.0	30
240	Magnetic dual-template molecularly imprinted polymer based on syringe-to-syringe magnetic solid-phase microextraction for selective enrichment of p-Coumaric acid and ferulic acid from pomegranate, grape, and orange samples. Food Chemistry, 2020, 325, 126902.	8.2	30
241	Simultaneous selective enrichment of methylparaben, propylparaben, and butylparaben from cosmetics samples based on syringe-to-syringe magnetic fluid phase microextraction. Talanta, 2021, 221, 121547.	5.5	30
242	Determination of Cu, Fe, Pb and Zn by Flameâ€AAS after Preconcentration Using Sodium Dodecyl Sulfate Coated Alumina Modified with Complexing Agent. Journal of the Chinese Chemical Society, 2009, 56, 150-157.	1.4	29
243	Ionic liquid-based dispersive liquid-liquid microextraction combined with high performance liquid chromatography-UV detection for simultaneous preconcentration and determination of Ni, Co, Cu and Zn in water samples. Journal of the Serbian Chemical Society, 2014, 79, 63-76.	0.8	29
244	Optimization of the combined ultrasonic assisted/adsorption method for the removal of malachite green by zinc sulfide nanoparticles loaded on activated carbon: experimental design. RSC Advances, 2015, 5, 100129-100141.	3.6	29
245	Application of ultrasonic radiation for simultaneous removal of auramine O and safranine O by copper sulfide nanoparticles: Experimental design. Spectrochimica Acta - Part A: Molecular and Biomolecular Spectroscopy, 2015, 136, 1069-1075.	3.9	29
246	Ultrasonic assisted dispersive solid-phase microextraction of Eriochrome Cyanine R from water sample on ultrasonically synthesized lead (II) dioxide nanoparticles loaded on activated carbon: Experimental design methodology. Ultrasonics Sonochemistry, 2017, 34, 317-324.	8.2	29
247	A highly selective nanocomposite based on MIP for curcumin trace levels quantification in food samples and human plasma following optimization by central composite design. Journal of Chromatography B: Analytical Technologies in the Biomedical and Life Sciences, 2017, 1040, 129-135.	2.3	29
248	A rapid and efficient sonophotocatalytic process for degradation of pollutants: Statistical modeling and kinetics study. Journal of Molecular Liquids, 2018, 261, 291-302.	4.9	29
249	Adsorption of nalidixic acid antibiotic using a renewable adsorbent based on Graphene oxide from simulated wastewater. Journal of Environmental Chemical Engineering, 2021, 9, 105975.	6.7	29
250	Simple and facile sonochemical synthesis of lead oxide nanoparticles loaded activated carbon and its application for methyl orange removal from aqueous phase. Journal of Molecular Liquids, 2016, 213, 48-57.	4.9	28
251	Ultrasound-assisted extraction of antimicrobial compounds from Thymus daenensis and Silybum marianum: Antimicrobial activity with and without the presence of natural silver nanoparticles. Ultrasonics Sonochemistry, 2018, 42, 76-83.	8.2	28
252	Magnetic metal organic framework for pre-concentration of ampicillin from cow milk samples. Journal of Pharmaceutical Analysis, 2020, 10, 365-375.	5.3	28

#	Article	IF	CITATIONS
253	Oxidized Multiwalled Carbon Nanotubes as Adsorbents for Kinetic and Equilibrium Study of Removal of 5-(4-Dimethyl Amino Benzylidene)Rhodanine. Arabian Journal for Science and Engineering, 2013, 38, 1691-1699.	1.1	27
254	Functionalization of multiwalled carbon nanotubes for the solid-phase extraction of silver, cadmium, palladium, zinc, manganese and copper by flame atomic absorption spectrometry. Human and Experimental Toxicology, 2013, 32, 687-697.	2.2	27
255	Extraction of ultra-traces of lead, chromium and copper using ruthenium nanoparticles loaded on activated carbon and modified with N,N-bis-(α-methylsalicylidene)-2,2-dimethylpropane-1,3-diamine. Mikrochimica Acta, 2015, 182, 1187-1196.	5.0	27
256	Combination of cloud point extraction and flame atomic absorption spectrometry for preconcentration and determination of trace iron in environmental and biological samples. Open Chemistry, 2008, 6, 488-496.	1.9	26
257	A Cloud Point Extraction Procedure for Preconcentration/Flame Atomic Absorption Spectrometric Determination of Silver, Zinc, and Lead at Subtrace Levels in Environmental Samples. Journal of AOAC INTERNATIONAL, 2009, 92, 907-913.	1.5	26
258	Application of Optimized Vortex-Assisted Surfactant-Enhanced DLLME for Preconcentration of Thymol and Carvacrol, and Their Determination by HPLC-UV: Response Surface Methodology. Journal of Chromatographic Science, 2015, 53, 1222-1231.	1.4	26
259	Efficient adsorption of Europhtal onto activated carbon modified with ligands (1E,2E)-1,2-bis(pyridin-4-ylmethylene)hydrazine (M) and (1E,2E)-1,2-bis(pyridin-3-ylmethylene)hydrazine (SCH-4); response surface methodology. RSC Advances, 2015, 5, 42376-42387.	3.6	26
260	Intensified removal of Malachite green by AgOHâ€AC nanoparticles combined with ultrasound: Modeling and optimization. Applied Organometallic Chemistry, 2017, 31, e3857.	3.5	26
261	Removal of Malachite Green Dye Using IRMOF-3–MWCNT-OH–Pd-NPs as a Novel Adsorbent: Kinetic, Isotherm, and Thermodynamic Studies. Journal of Chemical & Engineering Data, 2019, 64, 4801-4814.	1.9	26
262	Electrochemical synthesis of Zn:ZnO/Ni2P and efficient photocatalytic degradation of Auramine O in aqueous solution under multi-variable experimental design optimization. Polyhedron, 2019, 165, 1-8.	2.2	26
263	Adsorption of the azo dyes from wastewater media by a renewable nanocomposite based on the graphene sheets and hydroxyapatite/ZnO nanoparticles. Journal of Molecular Liquids, 2022, 350, 118568.	4.9	26
264	Silver nanoparticle loaded on activated carbon and activated carbon modified with 2-(4-isopropylbenzylideneamino)thiophenol (IPBATP) as new sorbents for trace metal ions enrichment. International Journal of Environmental Analytical Chemistry, 2013, 93, 386-400.	3.3	25
265	Dispersion of hydrophobic magnetic nanoparticles using ultarsonic-assisted in combination with coacervative microextraction for the simultaneous preconcentration and determination of tricyclic antidepressant drugs in biological fluids. Ultrasonics Sonochemistry, 2016, 32, 380-386.	8.2	25
266	Removal of methylene blue from aqueous solution by walnut carbon: optimization using response surface methodology. Desalination and Water Treatment, 2016, 57, 3179-3193.	1.0	25
267	A dual surface inorganic molecularly imprinted Bi2WO6-CuO/Ag2O heterostructure with enhanced activity-selectivity towards the photocatalytic degradation of target contaminantst. Photochemical and Photobiological Sciences, 2020, 19, 943-955.	2.9	25
268	Hydrophilic magnetic molecularly imprinted resin in PVDF membrane for efficient selective removal of dye. Journal of Environmental Management, 2021, 300, 113707.	7.8	25
269	Construction of Suitable Iodide–Selective Electrode Based on Phenyl Mercury (II)(2â€mercaptobezothiozolate) Carrier. Analytical Letters, 2007, 40, 1714-1735.	1.8	24
270	Simultaneous extraction and preconcentration of some metal ions using eucalyptus-wood based activated carbon modified with silver hydroxide nanoparticles and a chelating agent: optimization by an experimental design. RSC Advances, 2015, 5, 89204-89217.	3.6	24

#	Article	IF	CITATIONS
271	The choice of ultrasound assisted extraction coupled with spectrophotometric for rapid determination of gallic acid in water samples: Central composite design for optimization of process variables. Ultrasonics Sonochemistry, 2017, 34, 692-699.	8.2	24
272	Superhydrophobic–superoleophilic electrospun nanofibrous membrane modified by the chemical vapor deposition of dimethyl dichlorosilane for efficient oil–water separation. Journal of Applied Polymer Science, 2019, 136, 47621.	2.6	24
273	Gold anchoring to CuFe2F8(H2O)2 oxyfluoride for robust sono-photodegradation of Rhodamine-B. Journal of Cleaner Production, 2021, 313, 127916.	9.3	24
274	Kinetic and isotherm study of Bromothymol Blue and Methylene blue removal using Au-NP loaded on activated carbon. Desalination and Water Treatment, 2014, 52, 5504-5512.	1.0	23
275	Comparison of nickel oxide and palladium nanoparticle loaded on activated carbon for efficient removal of methylene blue. Human and Experimental Toxicology, 2015, 34, 153-169.	2.2	23
276	Simultaneous extraction and preconcentration of Cu2+, Ni2+ and Zn2+ ions using Ag nanoparticle-loaded activated carbon: Response surface methodology. Advanced Powder Technology, 2016, 27, 426-435.	4.1	23
277	Optimization of simultaneous ultrasound assisted toxic dyes adsorption conditions from single and multi-components using central composite design: Application of derivative spectrophotometry and evaluation of the kinetics and isotherms. Ultrasonics Sonochemistry, 2017, 36, 236-245.	8.2	23
278	A review on corona virus disease 2019 (COVID-19): current progress, clinical features and bioanalytical diagnostic methods. Mikrochimica Acta, 2022, 189, 103.	5.0	22
279	Artificial Neural Network (ANN) Method for Modeling of Sunset Yellow Dye Adsorption Using Nickel Sulfide Nanoparticle Loaded on Activated Carbon: Kinetic and Isotherm Study. Journal of Dispersion Science and Technology, 2015, 36, 1339-1348.	2.4	21
280	SnO2 nanoparticle-loaded activated carbon for simultaneous removal of Acid Yellow 41 and Sunset Yellow; derivative spectrophotometric, artificial neural network and optimization approach. Spectrochimica Acta - Part A: Molecular and Biomolecular Spectroscopy, 2015, 150, 1002-1012.	3.9	21
281	Adsorption of methyl red onto palladium nanoparticles loaded on activated carbon: experimental design optimization. Desalination and Water Treatment, 2016, 57, 22646-22654.	1.0	21
282	Amberlite XAD-7 resin impregnated with 2-(1-(4-chlorophenyl)-4,5-diphenyl-1H-imidazol-2yl)-4-nitrophenol for enrichment of metal ions. Journal of Saudi Chemical Society, 2014, 18, 674-680.	5.2	19
283	Application of an ionic-liquid combined with ultrasonic-assisted dispersion ofgold nanoparticles for micro-solid phase extraction of unmetabolized pyridoxine and folic acid in biological fluids prior to high-performance liquid chromatography. RSC Advances, 2015, 5, 70064-70072.	3.6	19
284	Adsorption of naphthalene onto high-surface-area nanoparticle loaded activated carbon by high performance liquid chromatography: response surface methodology, isotherm and kinetic study. RSC Advances, 2016, 6, 54322-54330.	3.6	19
285	Development of an eco-friendly approach based on dispersive liquid–liquid microextraction for the quantitative determination of quercetin in <i>Nasturtium officinale</i> , <i>Apium graveolens</i> , <i>Spinacia oleracea</i> , <i>Brassica oleracea var. sabellica</i> , and food samples. New lournal of Chemistry. 2018. 42. 14340-14348.	2.8	19
286	<p>Nanoporous solid-state membranes modified with multi-wall carbon nanotubes with anti-biofouling property</p> . International Journal of Nanomedicine, 2019, Volume 14, 1669-1685.	6.7	19
287	Processing Guar Gum into polyester fabric based promising mixed matrix membrane for water treatment. Carbohydrate Polymers, 2021, 254, 116806.	10.2	19
	Syntheses, crystal, and molecular structures of Mn(II), Zn(II), and Ce(III) compounds and solution		

288

studies of Mn(II), Ni(II), Cu(II), Zn(II), Cd(II), and Ce(III) compounds obtained from a suitable proton transfer compound containing bda and pydcH2 (bdaÂ=Âbutane-1,4-diamine;) Tj ETQq0 0 0 rgBT /Overlock 10 Tf 50^{20}_{52} Td (pydcH2Â=Âp

#	Article	IF	CITATIONS
289	Tin oxide nanoparticles loaded on activated carbon as adsorbent for removal of Murexide. Desalination and Water Treatment, 2014, 52, 7282-7292.	1.0	18
290	Simultaneous and rapid dye removal in the presence of ultrasound waves and a nano structured material: experimental design methodology, equilibrium and kinetics. RSC Advances, 2016, 6, 66311-66319.	3.6	18
291	Synthesis of CuS nanoparticles and evaluation of its antimicrobial properties in combination with <i>Linum usitatissimum</i> root and shoot extract. Desalination and Water Treatment, 2016, 57, 24456-24466.	1.0	18
292	Synthesis and characterization of antibacterial chromium iron oxide nanoparticleâ€loaded activated carbon for ultrasoundâ€assisted wastewater treatment. Applied Organometallic Chemistry, 2018, 32, e3981.	3.5	18
293	Potentiometric Ion-Selective Electrode Based on a New Single Crystal Cadmium(II) Schiff Base Complex for Detection of Fluoride Ion: Central Composite Design Optimization. IEEE Sensors Journal, 2019, 19, 413-425.	4.7	18
294	Corn derivative mesoporous carbon microspheres supported hydrophilic polydopamine for development of new membrane: Water treatment containing bovine serum albumin. Chemosphere, 2020, 259, 127440.	8.2	18
295	Adsorption performance of calcined copper-aluminum layered double hydroxides/CNT/PVDF composite films toward removal of carminic acid. Journal of Molecular Liquids, 2021, 329, 115558.	4.9	18
296	Thiocyanate-selective membrane electrode based on cobalt(III) Schiff base as a charge carrier. International Journal of Environmental Analytical Chemistry, 2008, 88, 841-856.	3.3	17
297	Preconcentration of Zn2+ and Cu2+ ions from food and vegetable samples using modified activated carbon. Environmental Monitoring and Assessment, 2012, 184, 6583-6591.	2.7	17
298	Antibacterial and antifungal activity of flower extracts of Urtica dioica, Chamaemelum nobile and Salvia officinalis: Effects of Zn[OH]2 nanoparticles and Hp-2-minh on their property. Journal of Industrial and Engineering Chemistry, 2015, 32, 353-359.	5.8	17
299	Preparation of chitosan functionalized endâ€capped Agâ€NPs and composited with Fe ³ O ⁴ â€NPs: Controlled release to pHâ€responsive delivery of progesterone and antibacterial activity against <i>pseudomonas aeruginosa (PAOâ€1)</i> . Applied Organometallic Chemistry, 2018, 32, e3921.	3.5	17
300	Comparative study of acid yellow 119 adsorption onto activated carbon prepared from lemon wood and ZnO nanoparticles loaded on activated carbon. Applied Organometallic Chemistry, 2018, 32, e4080.	3.5	17
301	A rapid and efficient sono-chemistry process for removal of pollutant: Statistical modeling study. Polyhedron, 2019, 171, 65-76.	2.2	17
302	Electrostatically controlled plasmonic effects of gold nanoparticles with indigo-carmine functionation for rapid and straightforward colorimetric detection of Cu2+ ions. Spectrochimica Acta - Part A: Molecular and Biomolecular Spectroscopy, 2020, 230, 118026.	3.9	17
303	Optimization of solid phase dispersive fieldâ€assisted ultrasonication for the extraction of auramine O and crystal violet dyes using central composite design. Applied Organometallic Chemistry, 2018, 32, e4181.	3.5	16
304	Degradation of Orange G and Trypan blue using Ag2C2O4/Ag/g-C3N4 composites as efficient photocatalyst under solar irradiation. Journal of Photochemistry and Photobiology A: Chemistry, 2020, 401, 112755.	3.9	16
305	Robust charge carrier by Fe3O4 in Fe3O4/WO3 core-shell photocatalyst loaded on UiO-66(Ti) for urea photo-oxidation. Chemosphere, 2021, 267, 129206.	8.2	16
306	Design of active photocatalysts and visible light photocatalysis. Interface Science and Technology, 2021, 32, 557-623.	3.3	16

#	Article	IF	CITATIONS
307	Spinning disc photoreactor based visible-light-driven Ag/Ag2O/TiO2 heterojunction photocatalyst film toward the degradation of amoxicillin. Journal of Environmental Management, 2022, 303, 114216.	7.8	16
308	solid phase for enrichment and determination of copper, nickel, chromium, and zinc ions in soil, plants, and mint water samples. Environmental Monitoring and Assessment, 2011, 174, 171-186.	2.7	15
309	Modified Carbon Paste Electrode for Pb ²⁺ Ion Determination: Response Surface Methodology. IEEE Sensors Journal, 2015, 15, 2974-2983.	4.7	15
310	Preparation of silver nanoparticle loaded on activated carbon and its application for removal of malachite green from aqueous solution. Synthesis and Reactivity in Inorganic, Metal Organic, and Nano Metal Chemistry, 2016, , 00-00.	0.6	15
311	Sonochemical incorporated of cytosine in Cu-H2bpdc as an antibacterial agent against standard and clinical strains of Proteus mirabilis with rsbA gene. Ultrasonics Sonochemistry, 2018, 44, 223-230.	8.2	15
312	Multiâ€responses optimization of simultaneous adsorption of methylene blue and malachite green dyes in binary aqueous system onto Ni:FeO(OH)â€NWsâ€AC using experimental design: derivative spectrophotometry method. Applied Organometallic Chemistry, 2018, 32, e4148.	3.5	15
313	Ultrasonically synthesis of Mn- and Cu- @ ZnS-NPs-AC based ultrasound assisted extraction procedure and validation of a spectrophotometric method for a rapid preconcentration of Allura Red AC (E129) in food and water samples. Ultrasonics Sonochemistry, 2018, 43, 52-60.	8.2	15
314	Synthesis of CuS and ZnO/Zn(OH) ₂ nanoparticles and their evaluation for in vitro antibacterial and antifungal activities. Applied Organometallic Chemistry, 2018, 32, e4398.	3.5	15
315	Lead (II) adsorption from aqueous solutions onto modified ag nanoparticles: Modeling and optimization. Environmental Progress and Sustainable Energy, 2016, 35, 743-749.	2.3	14
316	Synthesis of CuS nanoparticles loaded on activated carbon composite for ultrasoundâ€assisted adsorption removal of dye pollutants: Process optimization using CCDâ€RSM, equilibrium and kinetic studies. Applied Organometallic Chemistry, 2018, 32, e4350.	3.5	14
317	Switchable polarity solvents for preconcentration and simultaneous determination of amino acids in human plasma samples. New Journal of Chemistry, 2018, 42, 10007-10015.	2.8	14
318	Highly efficient adsorption of Naphthol Green B and Phenol Red dye by Combination of Ultrasound wave and Copperâ€Doped Zinc Sulfide Nanoparticles Loaded on Pistachioâ€Nut Shell. Applied Organometallic Chemistry, 2018, 32, e4369.	3.5	14
319	Colorimetric determination of F-, Br- and I- ions by Ehrlich's bio-reagent oxidation over enzyme mimic like gold nanoparticles: Peroxidase-like activity and multivariate optimization. Spectrochimica Acta - Part A: Molecular and Biomolecular Spectroscopy, 2020, 226, 117606.	3.9	14
320	Cold nanoparticle loaded activated carbon as novel adsorbent for the removal of Congo red. Indian Journal of Science and Technology, 2011, 4, 1208-1217.	0.7	14
321	Synthesis and crystal structure of Mn(II) and Hg(II) compounds and solution studies of Mn(II), Zn(II), Cd(II) and Hg(II) compounds based on piperazinediium pyridine-2,3-dicarboxylate. Journal of the Iranian Chemical Society, 2009, 6, 620-637.	2.2	13
322	Solid phase extraction of heavy metals on chemically modified silica-gel with 2-(3-silylpropylimino) 2013, 93, 843-857.	3.3	13
323	Gold Nanoparticles Loaded on Activated Carbon as Novel Adsorbent for Kinetic and Isotherm Studies of Methyl Orange and Sunset Yellow Adsorption. Journal of Dispersion Science and Technology, 2015, 36, 652-659.	2.4	13
324	Visibleâ€lightâ€driven photocatalytic degradation of fenpyroximate in rotating packed bed reactor using Fe ₃ O ₄ @PbS@Ni ₂ P magnetic nanocomposite photocatalyst: Response surface modelling and optimization. Applied Organometallic Chemistry, 2018, 32, e4513.	3.5	13

MEHRORANG GHAEDI

#	Article	IF	CITATIONS
325	Preparation, Characterization and First Application of Graphene Oxideâ€Metforminâ€Nickel for the Suzuki Crossâ€Coupling Reaction. ChemistrySelect, 2020, 5, 211-217.	1.5	13
326	Hierarchical Fe ₂ O ₃ /Na ₂ WO ₄ Nanofibers Supported on Conductive Carbon Cloth as a High-Performance Supercapacitor. Energy & Fuels, 2021, 35, 11551-11562.	5.1	13
327	Chemically modified nano silica gel with 2-((3silylpropylimino) methyl)-2-hydroxy-1-naphthol (SPIMHN) as good and efficient adsorbent for solid phase extraction. Desalination and Water Treatment, 2012, 41, 315-324.	1.0	12
328	Hydrophilic polymeric membrane supported on silver nanoparticle surface decorated polyester textile: Toward enhancement of water flux and dye removal. Chinese Journal of Chemical Engineering, 2020, 28, 901-912.	3.5	12
329	Biosorption. Interface Science and Technology, 2021, , 587-628.	3.3	12
330	Experimental design for the optimization of paraquat removal from aqueous media using a fixed-bed column packed with Pinus Eldarica stalks activated carbon. Chemosphere, 2022, 291, 132670.	8.2	12
331	Solid Phase Extraction and Spectrophotometric Determination of Trace Amounts of Thiocyanate in Real Samples. Annali Di Chimica, 2006, 96, 689-696.	0.6	11
332	Schiff Base Impregnated Plasticized Polyvinyl Chloride Optical Sensor for Selective and Efficient Detection of Copper (II) Ion: Central Composite Design. IEEE Sensors Journal, 2015, 15, 6604-6610.	4.7	11
333	Investigation of phytochemical and antimicrobial properties of <i>Linum usitatissimum</i> in presence of ZnO/Zn(OH) ₂ nanoparticles and extraction of euphol from <i>Euphorbia microsciadia</i> . Desalination and Water Treatment, 2016, 57, 20597-20607.	1.0	11
334	Simultaneous removal of Cu ²⁺ and Cr ³⁺ ions from aqueous solution based on Complexation with Eriochrome cyanineâ€R and derivative spectrophotometric method. Applied Organometallic Chemistry, 2018, 32, e3918.	3.5	11
335	Podophyllotoxin extraction from <scp><i>Linum usitatissimum</i></scp> plant and its anticancer activity against HTâ€29, Aâ€549 and MDAâ€MBâ€231 cell lines with and without the presence of gold nanoparticles. Applied Organometallic Chemistry, 2018, 32, e4024.	3.5	11
336	Effective determination of trace residues of glibenclamide in urine samples using dispersive micro solid-phase extraction and its final detection by chromatographic analysis. Analytical Methods, 2019, 11, 627-634.	2.7	11
337	The Solid Phase Extraction of Some Metal Ions Using Palladium Nanoparticles Attached to Silica Gel Chemically Bonded by Silica-Bonded N-Propylmorpholine as New Sorbent prior to Their Determination by Flame Atomic Absorption Spectroscopy. Scientific World Journal, The, 2012, 2012, 1-9.	2.1	10
338	Zinc Oxide Nanoparticles Loaded on Activated Carbon and Its Application for Adsorption Removal of Uric Acid. Synthesis and Reactivity in Inorganic, Metal Organic, and Nano Metal Chemistry, 2015, 45, 1387-1395.	0.6	10
339	Hemidirected Coordination Sphere on Novel Lead(II) Nano Coordination Polymer: Synthesis, Structural Characterization and DFT Calculation of [Pb(p-2-einh)ClO4(MeOH)2]n. Journal of Inorganic and Organometallic Polymers and Materials, 2016, 26, 197-207.	3.7	10
340	Chemometric assisted sonochemical dyes adsorption in ternary solutions onto Cu nanowires loaded on activated carbon. Journal of the Taiwan Institute of Chemical Engineers, 2017, 76, 115-125.	5.3	10
341	Design and construction of a new optical solid-state mercury(<scp>ii</scp>) sensor based on PVC membrane sensitized with colloidal carbon dots. New Journal of Chemistry, 2017, 41, 11533-11545.	2.8	10
342	Construction of molecularly imprinted nanoparticles by employing ultrasound waves for selective determination of doxepin from human plasma samples: Modeling and optimization. Biomedical Chromatography, 2019, 33, e4675.	1.7	10

#	Article	IF	CITATIONS
343	<p>Culture of dental pulp stem cells on nanoporous alumina substrates modified by carbon nanotubes</p> . International Journal of Nanomedicine, 2019, Volume 14, 1907-1918.	6.7	10
344	Experimental study and modeling of in vitro agrochemicals release from nanoporous anodic alumina. Chemical Papers, 2020, 74, 1997-2009.	2.2	10
345	Ag2C2O4 /Ag3PO4 composites as efficient photocatalyst for solar light driven degradation of dyes pollutants. Solid State Sciences, 2020, 109, 106390.	3.2	10
346	Photoelectro-Fenton/photocatalytic process for decolorization of an organic compound by Ag:Cd-1,4-BDOAH2 nano-photocatalyst: Response surface modeling and central composite design optimization. Journal of Molecular Liquids, 2021, 335, 113689.	4.9	10
347	Development of an Efficient Procedure for Determination of Copper, Zinc and Iron after Solid Phase Extraction on 3â€(1â€(1â€Hâ€Indolâ€3â€yl)à€3â€Phenylallyl)â€1Hâ€Indole Loaded on Duolite XAD 761. Journal Chemical Society, 2010, 57, 275-283.	of. t he Chi	nese
348	Thiol functionalised ionic liquid based xerogel: a novel and efficient support for the solid phase extraction of transition metal ions. International Journal of Environmental Analytical Chemistry, 2013, 93, 1525-1536.	3.3	9
349	Optimizing the biosorption of Bi ³⁺ ions by Streptomyces rimosus using experimental design and applicability in kinetics and isotherm modeling. RSC Advances, 2016, 6, 40287-40295.	3.6	9
350	Random forest model for removal of methylene blue and lead(II) ion using activated carbon obtained from Tamarisk. Desalination and Water Treatment, 2016, 57, 19273-19291.	1.0	9
351	Design a sensitive optical thin film sensor based on incorporation of isonicotinohydrazide derivative in sol–gel matrix for determination of trace amounts of copper (II) in fruit juice: Effect of sonication time on immobilization approach. Ultrasonics Sonochemistry, 2018, 42, 723-730.	8.2	9
352	A facile and selective approach for enrichment of l-cysteine in human plasma sample based on zinc organic polymer: Optimization by response surface methodology. Journal of Pharmaceutical and Biomedical Analysis, 2018, 149, 166-171.	2.8	9
353	Preconcentration of some trace metal ions on coated alumina modified by 1-((6-(-(2-hydroxynaphthalen-1-yl)methyleneamino) hexylimino) methyl) naphthalen-2-ol. Toxicological and Environmental Chemistry, 2011, 93, 860-872.	1.2	8
354	Ultrasonic treatment of wastewater contaminated with various dyes using tin oxide hydroxide nanoparticles loaded on activated carbon: Synthesis, performance, mechanism and statistical optimization. Applied Organometallic Chemistry, 2017, 31, e3860.	3.5	8
355	Application of copper sulfide nanoparticles loaded activated carbon for simultaneous adsorption of ternary dyes: Response surface methodology. Korean Journal of Chemical Engineering, 2018, 35, 1108-1118.	2.7	8
356	DNA-shaped silver(<scp>i</scp>) coordination polymer based micro-solid phase extraction for determination of Amaranth and Brilliant Blue FCF in food and water samples. Analytical Methods, 2019, 11, 618-626.	2.7	8
357	DFNS/PEI/Cu Nanocatalyst for Reduction of Nitro-aromatic Compounds. Catalysis Letters, 2021, 151, 1653-1662.	2.6	8
358	Photocatalytic activity based on electrospun nanofibers. Interface Science and Technology, 2021, 32, 625-672.	3.3	8
359	Preconcentration/Separation of Some Metal Ions Using Sodium Dodecyl Sulfate Coated Alumina Modified with Bis(5â€bromoâ€2â€hydroxyâ€benzaldehyde)â€2â€methylâ€1,5â€pentane Diimine (BBHBPDI) Prio Flameâ€AAS Determination. Chinese Journal of Chemistry, 2011, 29, 2141-2147.	r 40 7 Their	7
360	Comparison of Activated Carbon and Oxidized Multiwalled Carbon Nanotubes Modified with Bis(3-Nitrobenzylidene)-1,2-Ethanediamine for Enrichment of Trace Amounts of Some Metal Ions. Journal of AOAC INTERNATIONAL, 2012, 95, 1761-1767.	1.5	7

#	Article	IF	CITATIONS
361	Combination of solid-phase extraction and flame atomic absorption spectrometry for simultaneous preconcentration and determination of some heavy metals in real samples. Desalination and Water Treatment, 2014, 52, 5430-5441.	1.0	7
362	Improvement in the performance of a zinc ion-selective potentiometric sensor using modified core/shell Fe3O4@SiO2nanoparticles. RSC Advances, 2015, 5, 105925-105933.	3.6	7
363	The Use of Ultrasound in pipetteâ€ŧip solidâ€phase extraction based on CuS@ZnS@Fe ₃ O ₄ â€CNTs for preâ€concentration of tartrazine in water samples. Applied Organometallic Chemistry, 2018, 32, e4274.	3.5	7
364	Sonophotocatalytic treatment of diazinon using visible lightâ€driven Ce:Cuâ€1,4â€BDOAH ₂ photocatalyst in a batchâ€mode process: Response surface methodology and optimization. Applied Organometallic Chemistry, 2018, 32, e3962.	3.5	7
365	A molecularly imprinted polymer coupled with high-performance liquid chromatography-UV for the determination of albendazole in plasma and urine samples: CCD-RSM design. New Journal of Chemistry, 2018, 42, 15937-15945.	2.8	7
366	Removal of Acid Red 299 dye on gold nanoparticles loaded on activated carbon: kinetic and thermodynamic investigation of the removal process. Desalination and Water Treatment, 2014, 52, 5494-5503.	1.0	6
367	Effects of drought stress and superabsorbent polymer on morpho-physiological and biochemical traits of Caper (Capparis spinosa L.). Australian Journal of Crop Science, 2020, , 13-20.	0.3	6
368	A cloud point extraction procedure for preconcentration/flame atomic absorption spectrometric determination of silver, zinc, and lead at subtrace levels in environmental samples. Journal of AOAC INTERNATIONAL, 2009, 92, 907-13.	1.5	6
369	Platinum Nanoparticles Loaded on Activated Carbon as Novel Adsorbent for the Removal of Congo Red. E-Journal of Chemistry, 2012, 9, 63-74.	0.5	5
370	Photocatalytic degradation of disulfine blue using titanium dioxide nanoparticles under ultraviolet light irradiation: A response surface methodology approach. Environmental Progress and Sustainable Energy, 2016, 35, 1657-1663.	2.3	5
371	Ultrasoundâ€assisted dispersive microâ€solidâ€phase extraction using hydrophobic thiolated ionic liquids immobilized on gold nanoparticles for the preconcentration and determination of amino acids in human plasma samples. Separation Science Plus, 2018, 1, 419-429.	0.6	5
372	Rapid ultrasoundâ€assisted microextraction of atorvastatin in the sample of blood plasma by nickel metal organic modified with alumina nanoparticles. Journal of Separation Science, 2020, 43, 4469-4479.	2.5	5
373	Photocatalytic Activity of Supported Metal Nanoparticles and Single Atoms. Chemistry - A European Journal, 2021, 27, 17999-18014.	3.3	5
374	Electrocatalytic membrane containing CuFeO2/nanoporous carbon for organic dye removal application. Chemical Engineering Research and Design, 2022, 183, 345-356.	5.6	5
375	SYNTHESIS AND CHARACTERIZATION OF CADMIUM SULFIDE NANOPARTICLE–LOADED ACTIVATED CARBON AS A NOVEL ADSORBENT FOR EFFICIENT REMOVAL OF REACTIVE ORANGE 12. Chemical Engineering Communications, 2013, 200, 1071-1088.	5 2.6	4
376	Development of an indirectly suspended droplet for the extraction of hazardous phenols from environmental aqueous samples. Analytical Methods, 2016, 8, 6074-6081.	2.7	4
377	Fabrication of size controlled nanocomposite based on zirconium alkoxide for enrichment of Gallic acid in biological and herbal tea samples. Journal of Chromatography B: Analytical Technologies in the Biomedical and Life Sciences, 2018, 1087-1088, 14-22.	2.3	4
378	Design of novel and modified dual optode membrane based on carbon dots for both ultratrace copper(ii) and cobalt(ii): derivative spectrophotometric and central composite design study. New Journal of Chemistry, 2018, 42, 2590-2604.	2.8	4

#	Article	IF	CITATIONS
379	Magnetic Ag3PO4/Ag2CrO4/Fe/Fe3O4 quaternary composite for improved solar-driven photocatalytic degradation of cationic dyes under natural solar radiation. Journal of Photochemistry and Photobiology A: Chemistry, 2022, 428, 113856.	3.9	4
380	Stereochemically active lone pair on lead(II) nano 3D supramolecular network: Synthesis, structural characterization, thermal stability and DFT calculation of [Pb(p-2-minh)2]. Main Group Chemistry, 2016, 15, 197-208.	0.8	3
381	In vitro curcumin delivery and antibacterial activity of RuS 2 and RuO 2 nanoparticles loaded chitosan biopolymer. Applied Organometallic Chemistry, 2018, 32, e4035.	3.5	3
382	Application of novel copper organic material for facile microextraction of sodium valproate from human plasma samples: Experimental design optimization and isotherm study. Applied Organometallic Chemistry, 2018, 32, e3960.	3.5	3
383	Developing a new colorimetric bioassay for iodide determination based on gold supported iridium peroxidase catalysts. New Journal of Chemistry, 2020, 44, 5588-5597.	2.8	3
384	Application of Terminalia catappa wood-based activated carbon modified with CuO nanostructures coupled with H2O2 for the elimination of chemical oxygen demand in the gas refinery. Journal of Nanostructure in Chemistry, 2022, 12, 159-177.	9.1	3
385	Conductive Polymers in Green Analytical Chemistry. ACS Symposium Series, 0, , 1-37.	0.5	3
386	Application of nanostructure ZnLI 2 complex in construction of optical pH sensor. Applied Organometallic Chemistry, 2018, 32, e4143.	3.5	2
387	Application of artificial neural network for comparison and modeling of the ultrasonic and stirrer assisted removal of anionic dye using activated carbon supported with nanostructure material. Applied Organometallic Chemistry, 2018, 32, e4050.	3.5	2
388	Designing, modelling, and optimising amido black and Eosin B dyes adsorption on MWCNT/ZrO ₂ /Pb nanocomposites from aqueous solution by response surface methodology. International Journal of Environmental Analytical Chemistry, 2023, 103, 8032-8050.	3.3	2
389	Degradation of mono ethylene glycol wastewater by different treatment technologies for reduction of COD gas refinery effluent. International Journal of Environmental Analytical Chemistry, 0, , 1-20.	3.3	2
390	Synthesis and characterization of SnO ₂ /(NH ₄) ₂ ‣nCl ₆ nanocomposites loaded on activated carbon and its application for adsorption of methylene Blue and Orange G. Applied Organometallic Chemistry, 2018, 32, e3903.	3.5	1
391	Dispersive liquidâ€liquid microextraction based on the solidification of floating organic droplets for preconcentration of amino acids in human plasma samples. Separation Science Plus, 2018, 1, 650-659.	0.6	1
392	Recent Advances in Carbon Nanostructure-Based Electrochemical Biosensors for Environmental Monitoring. Critical Reviews in Analytical Chemistry, 2021, , 1-17.	3.5	1
393	Kinetic and isotherm study of Sudan black B removal. Toxicology and Industrial Health, 2016, 32, 1891-1901.	1.4	0
394	Ultrasonic treatment of water contaminated with various pollutants onto copper nanowires loaded on activated carbon using response surface methodology and artificial intelligent. Applied Organometallic Chemistry, 2017, 31, e3878.	3.5	0
395	Current heterogeneous catalytic processes for environmental remediation of air, water, and soil. Interface Science and Technology, 2021, , 443-498.	3.3	0
396	Cytotoxic Effect of Podophyllotoxin-Loaded Magnetic Nanoparticles on Proliferation of Colorectal (HT-29) and Breast (MCF-7) Cancer Cell Lines. Current Nanomaterials, 2022, 07, .	0.4	0

#	Article	IF	CITATIONS
397	Synthesis and Characterization of Photoâ€catalyst Ag ₂ S/WO ₃ and its Application for Crystal Violet Degradation in the Aqueous Medium. ChemistrySelect, 2022, 7, .	1.5	Ο
398	Frontispiece: Photocatalytic Activity of Supported Metal Nanoparticles and Single Atoms. Chemistry - A European Journal, 2021, 27, .	3.3	0